

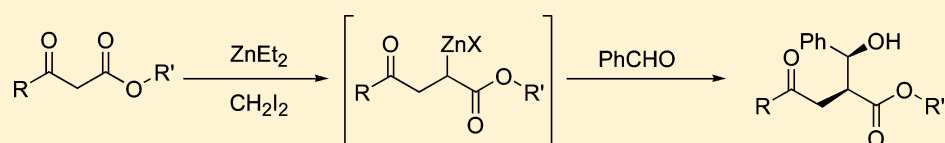
A Combined DFT and NMR Investigation of the Zinc Organometallic Intermediate Proposed in the *Syn*-Selective Tandem Chain Extension–Aldol Reaction of β -Keto Esters

Karelle S. Aiken,[†] Wilhelm A. Eger,[‡] Craig M. Williams,[‡] Carley M. Spencer,[†] and Charles K. Zercher^{*†}

[†]Department of Chemistry, University of New Hampshire, Durham, New Hampshire 03824, United States

[‡]School of Chemistry and Molecular Bioscience, University of Queensland, St. Lucia, Brisbane, QLD 4067, Australia

Supporting Information



ABSTRACT: The tandem chain extension–aldol (TCA) reaction of β -keto esters provides an α -substituted γ -keto ester with an average *syn:anti* selectivity of 10:1. It is proposed that the reaction proceeds via a carbon–zinc bound organometallic intermediate potentially bearing mechanistic similarity to the Reformatsky reaction. Evidence, derived from control Reformatsky reactions and a study of the structure of the TCA intermediate utilizing DFT methods and NMR spectroscopy, suggests the γ -keto group of the TCA intermediate plays a significant role in diastereoselectivity observed in this reaction. Such coordination effects have design implications for future zinc mediated reactions.

INTRODUCTION

A one-pot zinc carbenoid-mediated chain extension reaction in which β -keto esters **1** are converted to γ -keto esters **2** was first reported in 1997 (Scheme 1).¹ Further studies of this chain extension methodology have resulted in the chain extension of other substrates such as β -keto phosphonates and β -keto amides.² The originally proposed mechanism for this reaction³ involved formation of the classical donor–acceptor (push–pull) cyclopropane **4**, which fragments and forms intermediate **6** (via **5**), which on protonation provides chain-extended products (i.e., **2**). More recently, an extensive DFT study was performed to gain a better understanding of the mechanistic process, and an alternative pathway involving a cyclopropane transition state was also identified,⁴ which suggests that the presence of a cyclopropane intermediate (classical) and a cyclopropane transition state (nonclassical) are both viable.

Taking advantage of this proposed organometallic intermediate (**6**), a number of tandem reactions were subsequently developed (Scheme 2). Treatment of intermediate **6** with excess carbenoid in the presence of catalytic trimethylsilylchloride results in formation of an intermediate homoenolate (**7**), which can be quenched to provide α -methylated products (**8**) (Path A, Scheme 2).⁵ Alternatively, trapping the organometallic intermediate **6** with iodine, followed by elimination with base, provides a one-pot route for the generation of α,β -unsaturated γ -keto esters (**10**) (Path B, Scheme 2), which have been utilized in natural product synthesis.⁶ A tandem chain extension–aldol reaction, the primary focus of this report, provides *syn*-selective aldol products (**11**) (average dr 10:1)⁷ in equilibrium with the tetrahydrofuran hemiacetal forms (**12**) (Path C, Scheme 2).⁸ The tandem chain extension–aldol

reaction operates under kinetic control, consistent with the observation of increased diastereoselection at colder temperatures.⁷ In addition, these zinc carbenoid-mediated chain extension reactions provide efficient access to targeted materials involved in the synthesis of various natural products and natural product analogues.⁹ Chain extensions of amino acid-derived β -keto esters and β -keto amides have provided a number of ketomethylene isostere-containing dipeptide analogues.¹⁰

The intent of this study is to probe the nature of the common organometallic, reactive intermediate (i.e., **6**) involved in each of these above tandem reactions, with the goal of understanding the *syn*-selectivity in the second stage aldol reaction. Furthermore, insight into the nature of this common reactive intermediate will be important for future practitioners utilizing zinc reagents with a desired stereochemical outcome in mind.

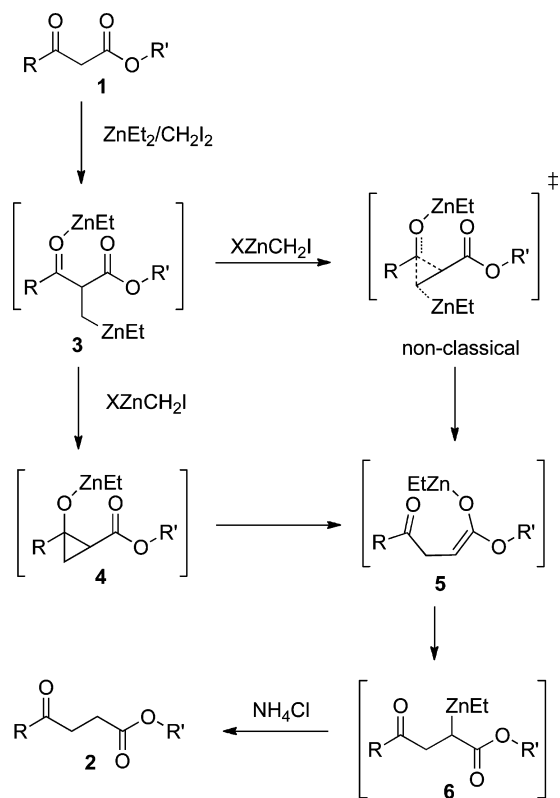
RESULTS AND DISCUSSION

In our earlier report, we suggested that the *syn* product of the TCA reaction results from the reaction of a *Z*-enolate,⁷ with the proposed preference for *Z*-enolate formation most likely related to the interplay between the ketone carbonyl and the organometallic intermediate (i.e., **6**). This intermediate, which functions as an enolate in the aldol reaction, appears to be similar to the reactive intermediate found in the traditional zinc-Reformatsky reaction (Scheme 3).¹¹

The zinc-Reformatsky intermediate is generated typically by zinc insertion into the carbon–halogen bond of a α -haloester

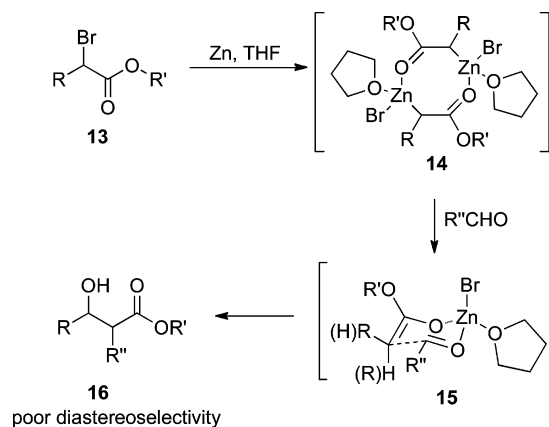
Received: March 13, 2012

Published: June 15, 2012

Scheme 1. Chain Extension Reaction of β -Keto Carbonyl Compounds

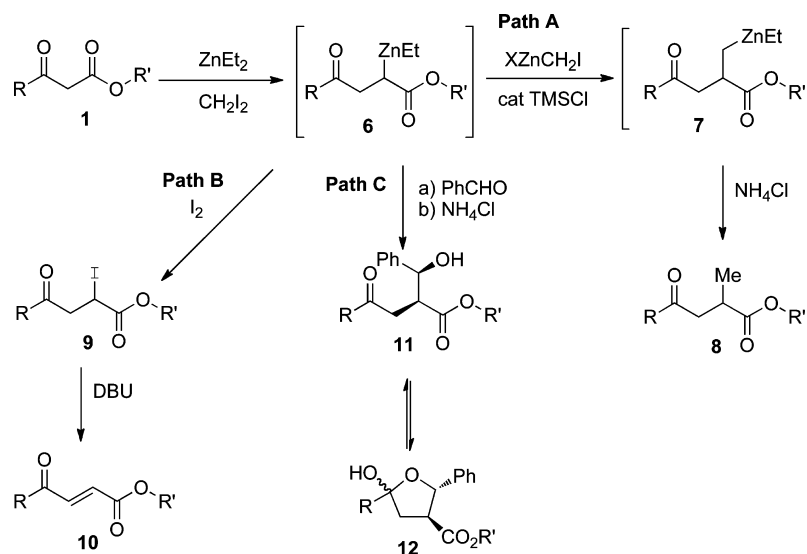
and has been extensively studied. X-ray crystallography and ebulliometry in THF have shown that the intermediate is a carbon-bound zinc organometallic structure, **14**, and that it exists as a dimer in both solution and its solid phase.^{11b} Observations made by ¹H and ¹³C NMR spectroscopy in a variety of coordinating solvents^{11a} have also shown the intermediate to possess a carbon-bound zinc. Using computational studies, Dewar et al. concluded that the carbon–zinc

Scheme 3. Zinc-Reformatsky Reaction

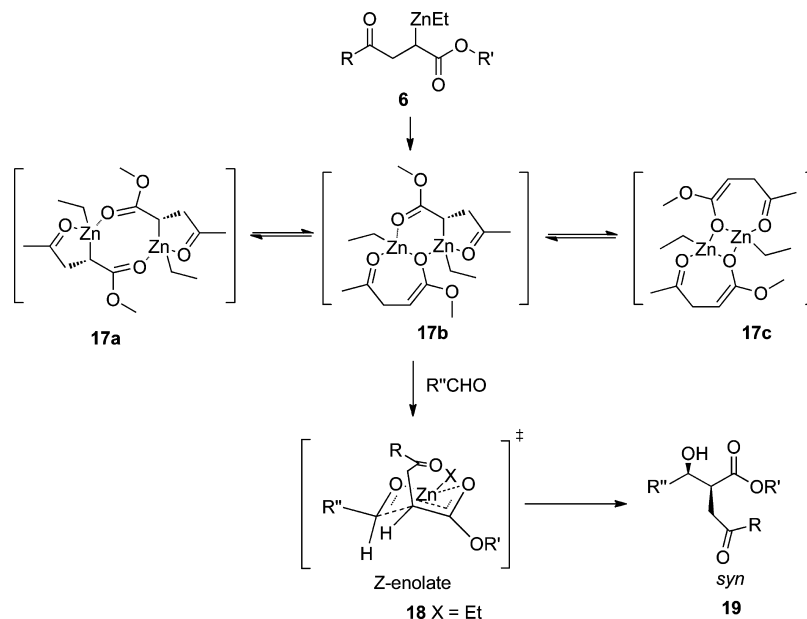
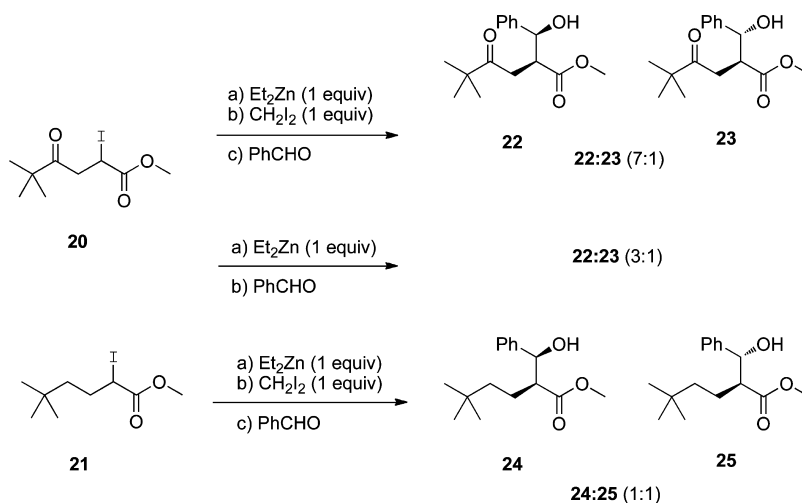


bound species **14** of the Reformatsky intermediate reacts with the aldehyde through its monomeric form.¹² It was further suggested that the more energetically favorable pathway for the reaction occurs via isomerization and a metallo-Claisen rearrangement of the enolate, a reaction which involves a six-electron, closed transition state **15**.

Unless performed in the presence of chiral functionality,¹³ the zinc-Reformatsky reaction provides poor *syn/anti* diastereoselectivity. This result stands in contrast to the tandem chain extension–aldol (TCA) reaction, which provides good *syn*-diastereocontrol (average dr 10:1), even though the only apparent difference between the two reactions is the presence of a γ -keto group in the proposed TCA intermediate (**6**). We initially proposed that the TCA reaction was proceeding through a monomeric form (via a metallo-Claisen rearrangement) in which complexation between the keto-carbonyl and Zn^{2+} biases the molecule toward the formation of a *Z*-enolate in preparation for the aldol reaction;⁷ however, a recent DFT study suggested that the structure of the TCA intermediate is dimeric, similar to that proposed for a zinc-Reformatsky reaction.⁷ Three possible dimeric structures (**17a**, **17b**, and **17c**) were calculated and are illustrated in Scheme 4.⁴

Scheme 2. Tandem Processes for the Chain Extension Reaction^a

^aPath A: α -methylation. Path B: α -iodination. Path C: aldol reaction.

Scheme 4. Proposed Structures for a Dimeric Form of the TCA Intermediate of β -Keto EstersScheme 5. Reformatsky Reactions of **20** and **21** and Tandem Chain Extension–Aldol Reaction of **25**

We present in this report: (1) a more detailed DFT study of the dimers in terms of stability and reactivity toward aldehydes; (2) experimentally determined reactivity data of the TCA intermediate as compared to the Reformatsky reaction; (3) spectroscopic evidence of a zinc intermediate; as well as (4) experimental and spectroscopic evidence that the interaction of the ketone with zinc is essential for *syn*-selectivity.

Control Study. In order to probe the role of the γ -keto group in the TCA reaction, control Reformatsky reactions were performed with two α -iodoesters, one with a γ -keto-group **20** and the other without a γ -keto group **21** (Scheme 5). Benzaldehyde was chosen as the aldehydic reaction partner for the reactions carried out at 0 °C in methylene chloride, which is the preferred solvent used for the zinc carbenoid-mediated chain extension reaction. Zinc insertion into the carbon–iodine bond of **20** and **21** was performed with diethylzinc, while diiodomethane was employed as an additive. The addition of diiodomethane in the control Reformatsky studies was intended to ensure that the reaction environment in the control study closely mimicked the ligand found on the

TCA intermediate. The ligand on intermediate **6** in the TCA reaction is unknown, since an ethyl group, an iodomethyl group, or other species resulting from decomposition of the zinc carbenoid could act as the ligand. Computational studies (*vide infra*) were performed with the ethyl group acting as a ligand due to the clear presence of ethylzinc moieties in NMR spectra. Structures have been drawn accordingly.

A Reformatsky reaction performed with α -iodo- γ -keto ester **20** resulted in the formation of products **22** and **23**, with a *syn:anti* ratio of 7:1. The importance of the added diiodomethane in this Reformatsky reaction was revealed through the observation of poor diastereocontrol when the reaction was performed in the absence of diiodomethane. Reaction of the substrate (**21**) that lacked the keto-group provided products **24** and **25** with a *syn:anti* ratio of 1:1, even in the presence of diiodomethane. These results were compared to the TCA reaction of **26** and benzaldehyde, which was reported previously and exhibited a *syn:anti* ratio of 12:1.⁷ It was postulated that both the TCA reaction of **26** and the Reformatsky reaction of **20** were proceeding through similar

intermediates, a γ -keto α -carbon-bound zinc organometallic ester **17**, while the reaction with **21** proceeded through a traditional Reformatsky intermediate **14**. The results of this control study strongly indicated that the γ -keto group of **20** was essential for the *syn*-selectivity of the aldol reaction. In turn, these results also suggested that the γ -keto group of the TCA intermediate **17** plays a large role in the *syn*-selectivity observed in the TCA reaction of β -keto esters like **26**.

NMR Study. Having verified a strong correlation between the γ -keto group of the TCA intermediate and the *syn*-selectivity of the aldol reaction, ^1H and ^{13}C NMR experiments were performed in order to determine whether the TCA intermediate (i.e., **6** or **17**) was indeed a carbon–zinc bound structure with a γ -keto- Zn^{2+} complexation. Initial attempts were made to generate a TCA-like intermediate from **20** and diethylzinc for NMR experiments (Figure 1). The intermediate

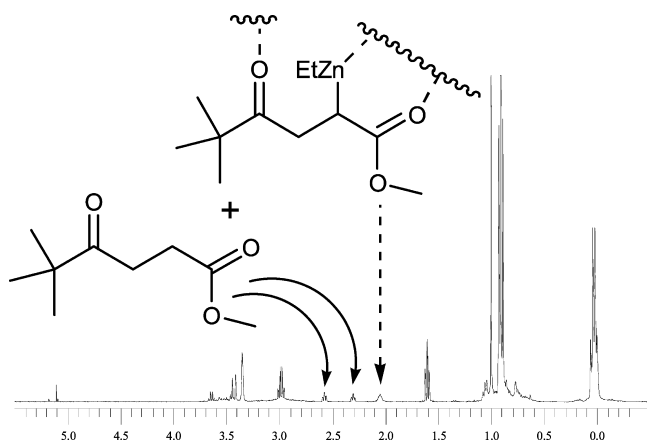


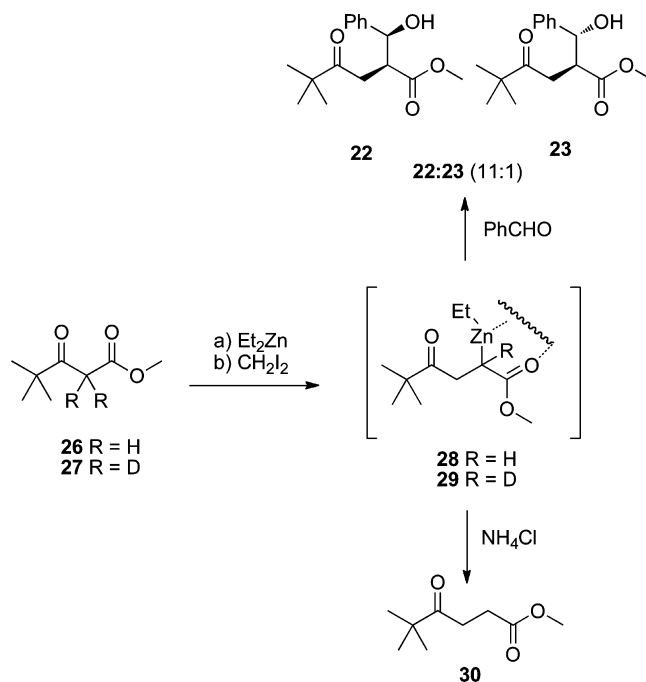
Figure 1. ^1H NMR spectra of the intermediate from **20**.

formed in this fashion would be formed in the absence of the carbenoid and its decomposition products, thus making its analysis easier. However, the intermediate generated by this method was not amenable to extensive spectroscopic experiments, as it converted to the γ -keto ester **30**¹⁴ within a few minutes of being formed, possibly through hydride delivery from the ethyl group. In Figure 1, the solid arrows are used to indicate the resonances of the two methylene units in **30**.

Eventually, the TCA intermediate was generated (Scheme 6) in CDCl_3 by sequential treatment of methyl pivaloylacetate **26** or its deuterated analogue **27** with 2 equiv of diethylzinc and 2 equiv of diiodomethane. The intermediate formed in this fashion was stable for up to 24 h, lending further support to the importance of the iodomethyl group in the intermediate. All spectra acquired from this intermediate were compared to ^1H and ^{13}C NMR spectra of the corresponding γ -keto ester **30** and to those reported in the literature for zinc-Reformatsky intermediates.¹¹

The ^1H NMR spectrum of the intermediate generated by treatment of methyl pivaloylacetate **26** with diethylzinc and diiodomethane was similar to that of the intermediate generated from **20**, although the resonances occurred at slightly different chemical shifts (Figure 1 vs Figure 2a). Most notable was the presence of a broad resonance in both spectra at 2.05 ppm in Figure 1 and at 2.66 ppm in Figure 2a. The occurrence of the broad resonance, in addition to singlets for the methyl ester, suggested that the intermediate generated in the study of the Reformatsky reaction with **20** was similar,

Scheme 6. Chain Extension Reactions of **26**



albeit not completely identical, to the intermediate of the TCA reaction.

The methyl ester and *t*-butyl protons of the TCA intermediate **28** could be easily assigned at 3.70 and 1.24 ppm, respectively (Figure 2a,b). The assignments for the α -methine and β -methylene protons proved to be more of a challenge; therefore, an experiment with α -deuterated methyl pivaloylacetate **27** was employed (Figure 2b). The proposed mechanism (Scheme 1) suggests chain extension of **27** would provide an intermediate (**29**) in which deuterium is incorporated α to the ester. The absence of a ^1H NMR resonance at 2.66 ppm when using the deuterated starting material indicated this resonance corresponded to the methine of the TCA intermediate **28**. The methylene protons were assigned as a broad resonance between 2.80 and 4.00 ppm through the use of 2D NMR experiments. These broadened resonances became more discernible in variable temperature NMR investigations of the intermediate (Figure 3).

The broadness of the methine and methylene resonances was proposed to result from a dynamic process in which intermediate exchange was being observed on the NMR time-scale at room temperature. Whether this was an intermolecular or intramolecular dynamic process could not be verified. A variable temperature study was employed in an effort to approach slow exchange and determine the number of the various intermediate species that existed. The lowest temperature at which useful data could be obtained was $-15\text{ }^\circ\text{C}$, a temperature at which the intermediate approached slow exchange as the broad methylene resonance between 2.80–4.00 ppm resolved into two resonances at 3.71 and 2.97 ppm. The methine resonance at 2.66 ppm also resolved into two resonances at 2.71 and 2.58 ppm with an approximate integral ratio of 4:1, respectively.

At 0 and $-15\text{ }^\circ\text{C}$, the signals at 3.71 and 2.91 ppm each integrated for one proton relative to the sum of the integrals for the methine protons at 2.71 and 2.58 ppm. In view of this integral ratio, the decoalescence of the resonance for the

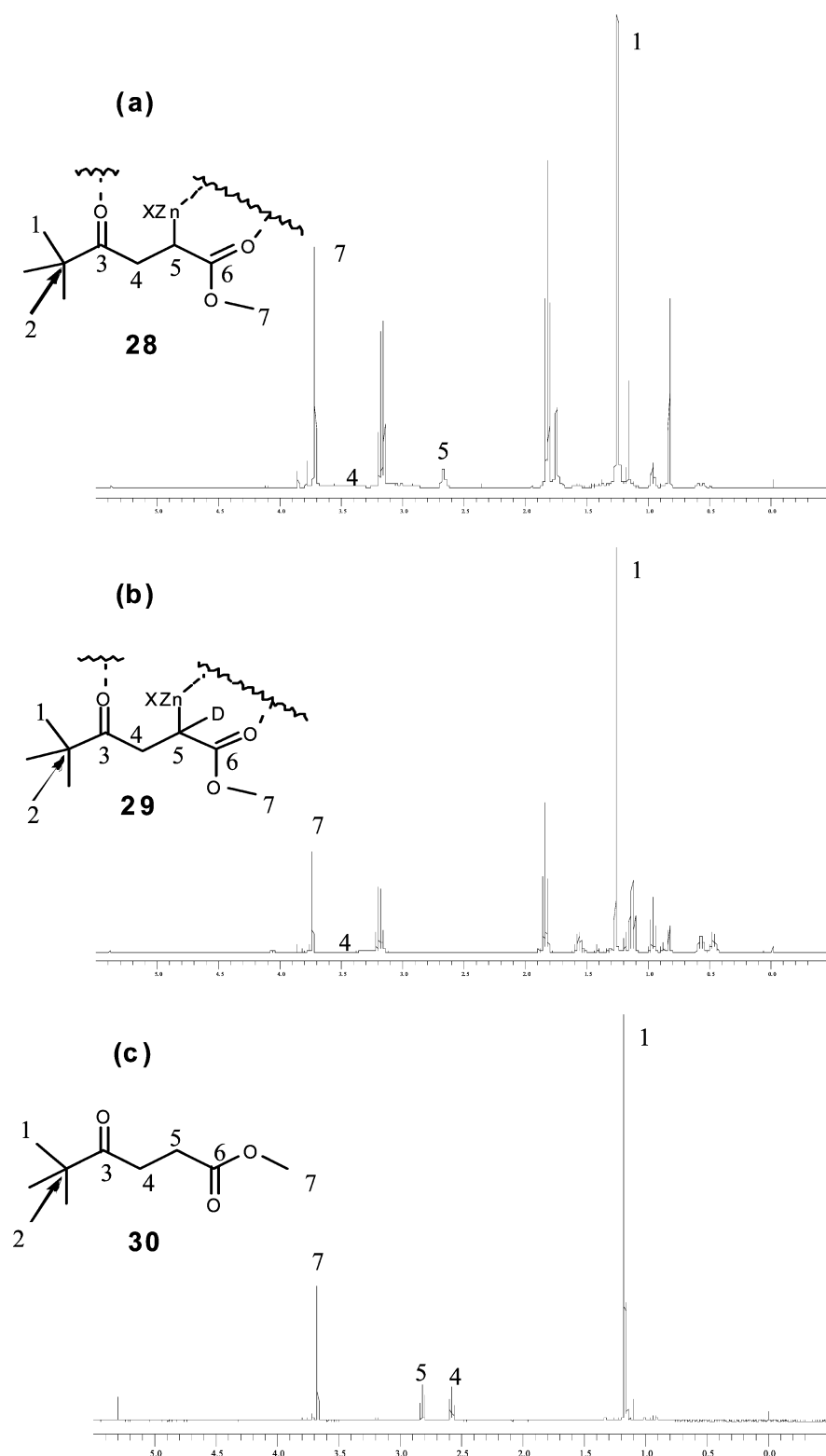


Figure 2. Identification of the organometallic's methine resonance. ^1H NMR spectra of (a) **28**; (b) **29**; (c) **30**.

methylene protons at 3.25 ppm (19°C) into resonances at 3.71 and 2.91 ppm (0°C), appeared to be a separation of signals for diastereotopic methylene protons, as opposed to signals representing different zinc-organometallic species. The decoalescence of the methine resonances into two methine resonances at low temperature suggests that at least two distinct organometallic intermediates exist in solution. This

dynamic process was not reported in the NMR studies of the Reformatsky intermediate,¹¹ lending further support to the importance of the ketone in the dynamic process. The monomeric, dimeric, or oligomeric nature of these species is unknown. No differences were observed in the NMR spectra of the intermediate generated at different concentrations.

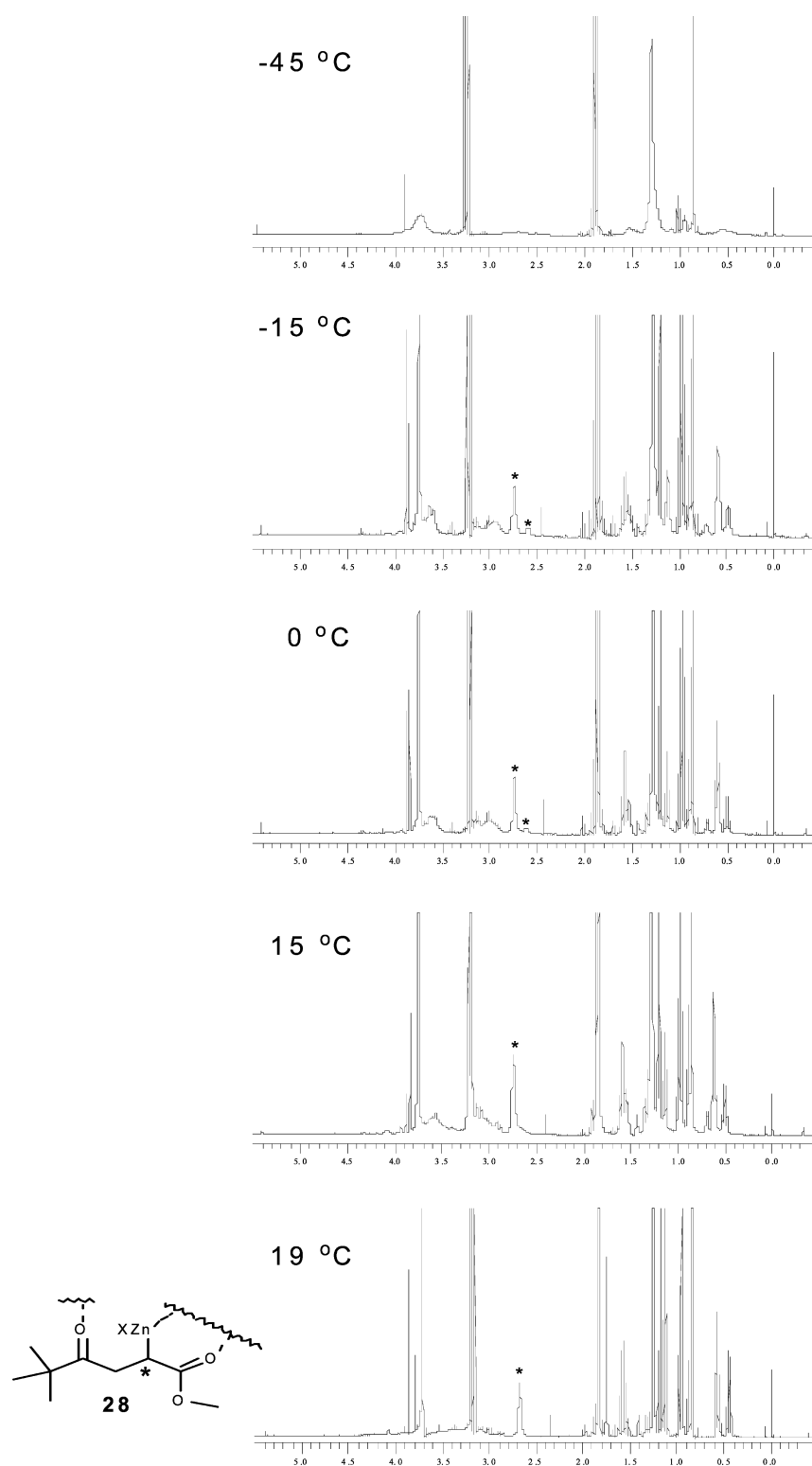


Figure 3. Variable temperature NMR study of intermediate **28**.

More insight into the structure of the TCA intermediate was obtained with ^{13}C NMR experiments (Figure 4). The ^{13}C NMR spectrum of this intermediate (**28**) exhibited chemical shifts for the ketone and the ester carbonyls at 230.0 and 184.9 ppm, respectively. Importantly, both chemical shifts were downfield of the corresponding functional groups in the γ -keto ester **30**, which resonated at 214.3 and at 173.7 ppm, respectively. The downfield shift of the carbonyls' resonances

suggests complexation of Zn^{2+} species in solution. Other resonances corresponding to the TCA intermediate were assigned through the use of DEPT and 2D NMR experiments (Table 1).

The use of THF as an additive provided further evidence that linked Zn^{2+} complexation of the TCA intermediate's ketone carbonyl to the 10:1 *syn*-selectivity of the TCA reaction. When 5.4 equiv of THF was added to the intermediate, the ^{13}C NMR

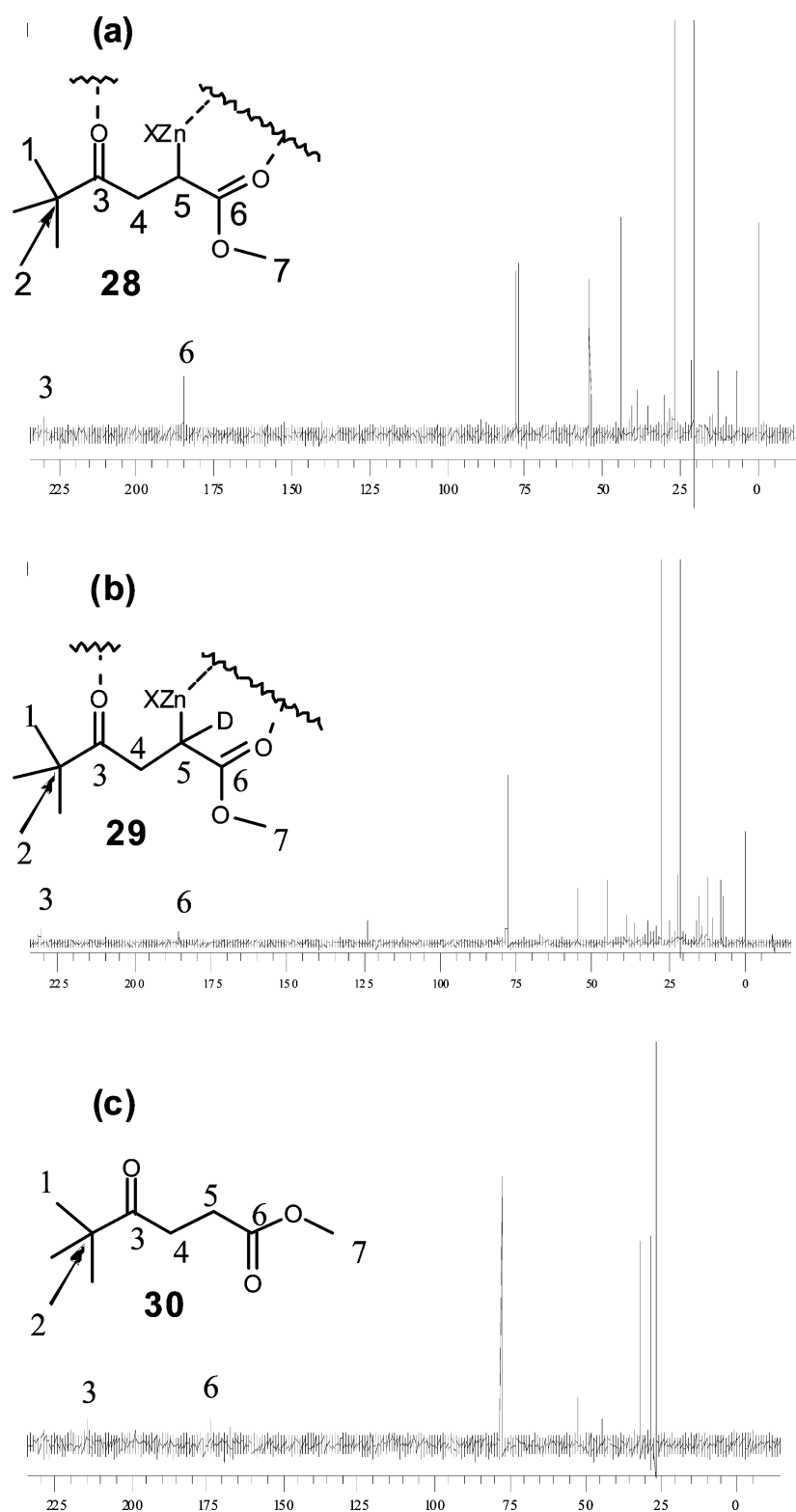
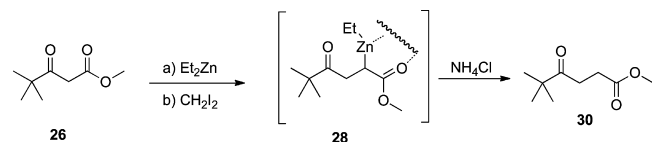


Figure 4. Effect of the zinc organometallic on the chemical shift of the ketone's carbonyl. ^{13}C NMR spectra of (a) **28**; (b) **29**; (c) **30**.

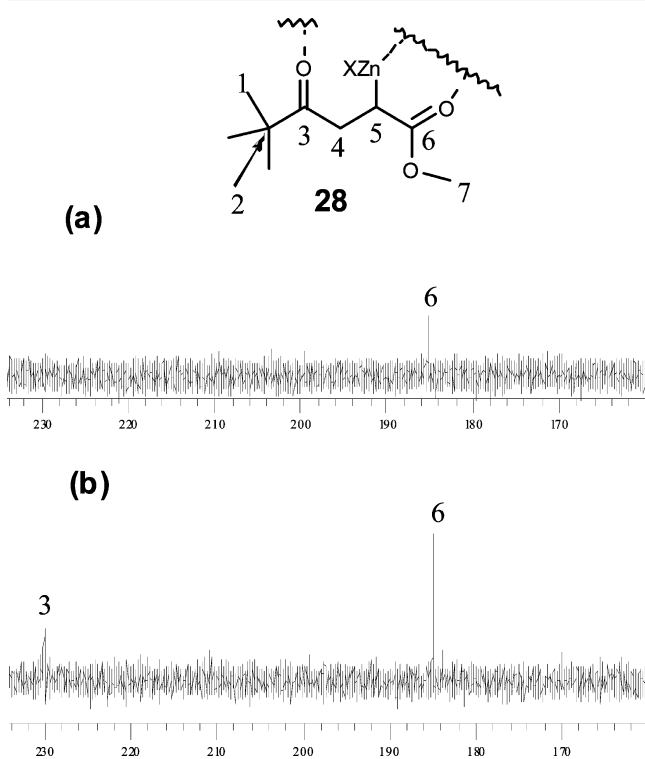
spectrum exhibited a disappearance in the ketone's carbonyl resonance at 230 ppm (Figure 5). The resonance for the ester carbonyl was unaffected by the presence of THF. This result suggested that the ester functionality in the intermediate forms a stable complex with Zn^{2+} , which is unperturbed by the presence of the THF donor. This stable complex involving the ester functionality is reminiscent of the Reformatsky

intermediate, which is also unaffected by the presence of donor solvents.¹⁰ Absence of the ketone's resonance suggested that THF may be competing with the ketone for the remaining site on the tetracoordinate Zn^{2+} . In theory, the uncomplexed ketone should exhibit a resonance at approximately 214 ppm, a chemical shift similar to that of the ketone resonance found in **30**. The spectrum of the intermediate with added THF is

Table 1. Nuclear Magnetic Resonance Spectroscopy of 28: Assignments for Chemical Shifts



| nucleus | ¹ H NMR | | | | nucleus | ¹³ C NMR | |
|---------|--------------------|-------|------|------|---------|---------------------|-------|
| | 28 | | 30 | | | 28 | 30 |
| | δ | mult | δ | mult | | δ | δ |
| H1 | 1.24 | s | 1.15 | s | C1 | 26.7 | 26.7 |
| H4 | 2.80–4.00 | broad | 2.80 | t | C2 | 44.1 | 44.1 |
| H5 | 2.66 | broad | 2.55 | t | C3 | 230.0 | 214.3 |
| H7 | 3.70 | s | 3.65 | s | C4 | 38.5 (broad) | 28.2 |
| | | | | | C5 | 34.9 (broad) | 31.7 |
| | | | | | C6 | 184.9 | 173.7 |
| | | | | | C7 | 53.8 | 51.9 |

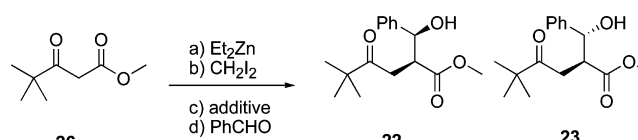
Figure 5. ¹³C NMR spectra of the carbonyl region of 28 (a) with 5.4 equiv of THF and (b) without THF.

consistent with a dynamic relationship between a complexed and uncomplexed ketone. Once again, this proposed Zn²⁺–ketone complexation could be inter- or intramolecular in nature.

Quenching of the TCA intermediate was performed with benzaldehyde in the absence and presence of THF (Table 2). A *syn:anti* (22:23) selectivity of 7:1 was observed when benzaldehyde was added to a solution that lacked THF. However, in the presence of 5.4 equiv of THF, an erosion of the *syn:anti* ratio to 3.3:1 was observed, a ratio more consistent with a typical Reformatsky reaction of a α -halo ester.¹³ This study provides additional support to the hypothesis that Zn²⁺–ketone complexation is involved in the *syn*-selectivity of the TCA reaction.

Concentration and Stereoselectivity. An investigation of the reaction concentration also provided insight into the TCA

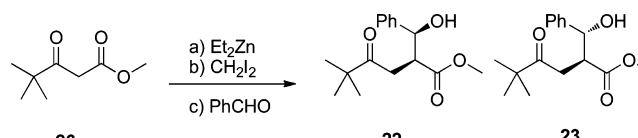
Table 2. Effects of THF Addition on the Stereoselectivity of the TCA Reactions



| [26] | additive | time/min | 22:23 <i>syn:anti</i> |
|------|------------------|----------|-----------------------|
| 0.34 | none | 60 | 7:1 |
| 0.34 | 5.4 equiv of THF | 60 | 3.3:1 |

reactions with benzaldehyde (Table 3). The *syn:anti* selectivity of these quenches is dependent on the concentration of the

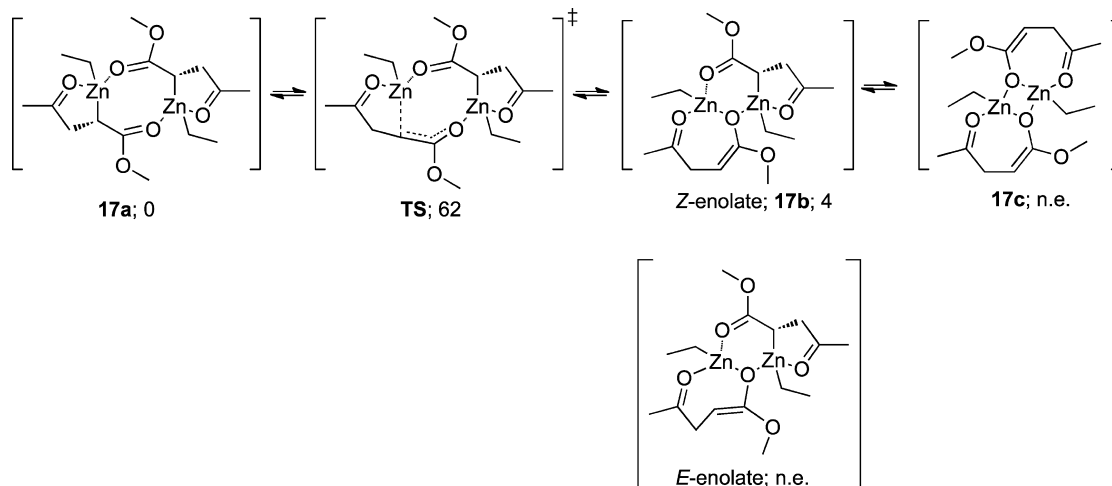
Table 3. Effect of Substrate Concentration on the Stereoselectivity of the TCA Reactions



| [26] | time/min | 22:23 <i>syn:anti</i> |
|-------|----------|-----------------------|
| 0.032 | 60 | 11:1 |
| 0.078 | 60 | 11:1 |
| 0.34 | 60 | 7:1 |

substrate, in that stereoselectivity decreases as the concentration of the substrate increases.

The original study of the TCA reaction had been performed with a substrate concentration of 0.08 M in methylene chloride.⁷ The chain-extended aldol product derived from 26 and benzaldehyde at this concentration had a *syn:anti* ratio of 12:1. During the NMR investigation of the zinc-organometallic intermediate (28), the concentration of methyl pivaloylacetate was 0.34 M in CDCl₃. While *syn* stereoselectivity on the order of a 7:1 ratio was still observed, this selectivity was significantly lower than the 12:1 ratio observed in the preparative-scale study of Lai.⁷ We undertook an NMR study of the TCA reaction at various substrate concentrations. No discernible differences in the organometallic intermediate were observable when comparing the ¹H NMR and ¹³C NMR spectra acquired at the concentrations of 0.34 and 0.08 M. However, upon addition of benzaldehyde to the 0.08 M reaction mixture, a

Scheme 7. Keto-Enol Tautomerization Step of the Dimeric Structure^a

^aGiven numbers are Gibbs free energies relative to 17a and in kJ/mol.

syn:anti selectivity of 11:1 was observed. This diastereomeric ratio was higher than that observed when the reaction was performed at 0.34 M and was closer to the *syn:anti* ratio of 12:1 that was observed in the original preparative scale study. An NMR tube experiment performed with a more dilute reaction mixture (0.032 M) also provided the TCA products in a *syn:anti* ratio of 11:1.

The diastereoselectivities observed at the various substrate concentrations reveal a concentration dependence on the selectivity of the TCA reaction, although the identical diastereoselectivities of the reactions at 0.03 and 0.08 M suggests a limit to substrate-concentration effects. Changing the concentration may affect the extent to which the intermediate's monomers aggregate, although the similarities of the intermediates' NMR spectra for the organometallic intermediates generated at different concentrations suggests that the fundamental structure of this aggregate is not greatly affected. The more concentrated solution (0.34 M) would favor increased intermolecular aggregation via the ketone carbonyl. Since the ketone carbonyl has been implicated in the *syn*-selectivity of the aldol reaction, enhanced aggregation involving the ketone might be expected to negatively impact the diastereoselectivity of the TCA reaction. Therefore, erosion in the *syn*-selectivity when using more concentrated reaction mixtures is consistent with the involvement of the ketone in the diastereocontrol of the aldol reaction.

DFT Study. NMR results described above reveal the presence of an organometallic aggregate in the TCA reaction, and previous calculations revealed that dimerization provides a significant gain in free energy in comparison to the correspondent monomeric structures.⁴ Therefore, the calculations presented in this body of work concentrate solely on dimeric structures. To simulate the reaction conditions most efficiently, the aldol reaction mechanism has been calculated including C-PCM solvent effects resembling dichloromethane, which is also the solvent used in the experimental investigations. In comparison to the gas phase model, the C-PCM calculations predict activation barriers to change significantly and reaction energies to be on average 10 kJ/mol lower (Table S1, Supporting Information). Major structural changes could only be observed at certain Zn–C or Zn–O coordination interactions, which became weaker

because of increased stabilization by the solvent. However, the results show that the inclusion of solvent effects is mandatory for understanding selectivity outcomes. For reduction in calculation time, the iodomethyl residue resulting from the Furukawa reagent as implemented in our earlier work has been exchanged to an ethyl residue, as it is not expected to participate in the aldol reaction mechanism. The reaction steps leading up to the inserted carbene moiety in the TCA pathway have been investigated thoroughly;⁴ therefore, the theoretical study herein will focus specifically on the reaction sequence starting from the chain-elongated intermediate.

First, the keto–enol tautomerization step, which theoretically can yield either *Z*- or *E*-enolates (Scheme 7), was calculated. The structure of the *E*-enolate (Scheme 7) could not be located at all because of the small interatomic distance between the carbon atom of the double bond and the zinc ion. As a result, this structure immediately relaxes to a *Z*-enolate, and thus only pathways following 17b have been calculated. In agreement with the findings of the ¹H NMR study, two stable intermediates for the tautomerization step have been found: structure 17a and the *Z*-enolate 17b, containing one enol and one keto tautomer, are energetically similar. Thus, no thermodynamic driving force is apparent for the reaction at this point. However, it should be noted that gas phase calculations predict 17b to be 11 kJ/mol more stable than 17a (Supporting Information). The transition state (TS), which proceeds along the carbon zinc bond, possesses an activation barrier of 62 kJ/mol relative to 17a and thus is easily surmountable. Furthermore, the predicted coordination between the zinc and the ketone group is also supported by these calculations. Additionally, a conceivable structure 17c (Scheme 7) containing two enolate moieties could not be located because of spontaneous relaxation to 17b. Thus only reaction pathways starting from 17b have been taken into account.

For conservation of computational time, but to still encompass substitution effects, acetaldehyde was used to evaluate the aldehyde addition reaction. Calculations demonstrate that the reaction proceeds via a one-step six-membered transition state, in which the oxygen of the acetaldehyde is coordinated to one of the zinc ions of 17b. As illustrated in Figure 6, these zinc ions have different coordination environ-

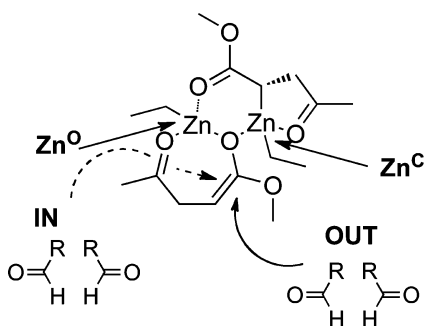


Figure 6. Overview of available options for nucleophilic attack by **17b** on acetaldehyde.

ments, namely, carbon (right, Zn^{C} , Figure 6) or oxygen (left, Zn^{O}) bound. In addition to these distinctions, the attack of the aldehyde can occur from two different sides of the double bond: (i) approach from the outer sphere (**OUT**, Figure 6), or (ii) approach from the inner sphere (**IN**), which is sterically encumbered by the other monomer. As shown below, a transition state derived from the (**IN**) approach is not automatically less stable. Furthermore, because of the unsymmetrical substitution pattern of the two zinc atoms, acetaldehyde can react through complexation with either zinc atom via four reaction paths involving variations in the facial selectivities of both the aldehydes and the enolate. (Figure 6).

The possible reaction products resulting from these pathway combinations are *syn* (S,R ; R,S) and *anti* (S,S ; R,R) esters. The configuration of the carbon derived from the aldehyde clearly depends on the methyl position during the course of reaction, whereas the configuration at the carbon of the former double bond of the enolate **17b** is related to the direction of aldehyde approach (**OUT** or **IN**, Table 4).

Table 4. Reaction Free Energies Relative to the Product Distribution in kJ/mol

| entry | attack possibilities ^a | | | TS ^b | IM ^c | product ^d | |
|-------|-----------------------------------|-----------|-----------|-----------------|-----------------|----------------------|-------------|
| 1 | Zn^{C} | IN | <i>Si</i> | 86 | 5 | R^e, R^f | <i>anti</i> |
| 2 | | | <i>Re</i> | 78 | 3 | R,S | <i>syn</i> |
| 3 | OUT | | <i>Si</i> | 88 | 17 | S,R | <i>syn</i> |
| 4 | | | <i>Re</i> | 85 | 17 | S,S | <i>ant</i> |
| 5 | Zn^{O} | IN | <i>Si</i> | 62 | -14 | S,R | <i>syn</i> |
| 6 | | | <i>Re</i> | 77 | 33 | S,S | <i>anti</i> |
| 7 | OUT | | <i>Si</i> | 84 | 43 | R,R | <i>anti</i> |
| 8 | | | <i>Re</i> | 69 | 14 | R,S | <i>syn</i> |

^aReaction possibilities ordered by (i) coordinating zinc ion, (ii) direction of aldehyde attack, (iii) attacking face of acetaldehyde.

^bReaction free energies of the transition states (TS). ^cReaction free energies of the intermediate states (IM), i.e., before quenching.

^dConfiguration of quenched products. ^eConfiguration of the carbon atom of the former double bond. ^fConfiguration of the carbon atom of the former acetaldehyde.

Reflecting on the activation barriers (TS) given in Table 4, aldehyde attack via the Zn^{O} coordination mode is on average slightly more favorable. That being said, all activation barriers seem surmountable, although the lowest barriers are associated with the *syn* products (Table 4, entries 5 and 8). Since the products are not formed until after the reaction is quenched following the aldehyde addition step, the energetics of the reaction intermediates are key to understanding the stereochemical course of the reaction, as opposed to product free

energies. Only one pathway of the reaction, leading to the favored *syn* product, is exergonic (Table 4, entry 5). The low energy barriers indicate the potential for reversibility and suggest that the reaction could be operating under thermodynamic control; however, experimental results appear to support kinetic control of the reaction.⁷

The reaction pathway with the lowest activation barrier leading to *syn* intermediate (Table 4, entry 5) and the equivalent pathway to *anti* (Table 4, entry 6) IM have been chosen for detailed discussion (Figure 7). In the initial *Zn*-enolate, the enolate oxygen is still bound to Zn^{O} but already slightly complexed to Zn^{C} . If acetaldehyde enters the dimer complex and the reaction starts, the enolate oxygen changes its coordination to Zn^{C} in favor of substrate acetaldehyde coordinating to Zn^{O} (Figure 7, TS). In the transition state, the C–C bond is formed simultaneously with the change in coordination of oxygen from Zn^{C} to Zn^{O} . Thus in IM, the oxygen of the former substrate acetaldehyde is bound to Zn^{O} .

Obviously, the only difference between both pathways is the configuration at the central carbon atom of the former substrate acetaldehyde (green layer). Depending on this configuration, the methyl group X points either to the outer (Table 4, entry 5, *syn*) or inner sphere (Table 4, entry 6, *anti*) of the dimeric system. Thus, steric repulsion increases activation barriers and reaction energies of entry 6 (Table 4). Because of the sp^3 hybridization of the former acetaldehyde carbon center and the orientation of the methyl group X, the central carbon atom of the former substrate acetaldehyde (green layer) can reach into the inner sphere in entry 5 (Table 4). This conformation results in a more relaxed CCO angle and thus in a more stable structure of the dimeric system. In entry 6 (Table 4), the former acetaldehyde forces the reacted monomer to point more toward the inner sphere resulting in a significant increase of steric tension. Furthermore, the methyl group Y (Figure 7) is able to rotate about 180° in entry 5 (IM) (Table 4) because of less steric repulsion.

Such impacts on the energetics discussed above can also be observed in the case of **OUT** attack. However, the resulting activation barriers and reaction energies are less favorable. In the case of the **OUT** intermediate structures (Table 4, entries 7 and 8), the nonreactive keto monomer unit and the zinc-coordinated sp^2 -hybridized ester group form a rigid ring structure. In contrast, coordination of the OMe portion of the ester group (Table 4, entries 1 and 2) in the **IN** intermediates allows for conformational relaxation resulting in a decrease in activation barriers and reaction energies of about ~ 10 kJ/mol. Thus, energetic asymmetry is created, and *syn* intermediate products are favored.

In the case of the Zn^{C} derived intermediate structures, entries 3 and 4 (Table 4) already form a pure enolate from the nonreacting keto monomer unit by breaking the Zn–C bond. In contrast, the still existent Zn–C interaction in entries 1 and 2 (Table 4) (illustrated in Figure 8) explains the significant energy difference to the **OUT** intermediates (entries 3 and 4). For steric reasons, arising mainly from lower angle of the sp^3 -hybridized carbon atom of the former aldehyde (in contrast to the flat sp^2 -hybridized carbon atom of the ester group), the **OUT** products (Table 4, entries 3 and 4) are not able to form this Zn–C bond. Facial selectivity of the acetaldehyde exerts no significant influence, as both intermediate structures (*Si*, *Re*) of each attack (**OUT**, **IN**) possess similar free energies. In contrast to Zn^{O} , the distinct positions of the methyl group are energetically inert (Figure 8). Furthermore, exchange between

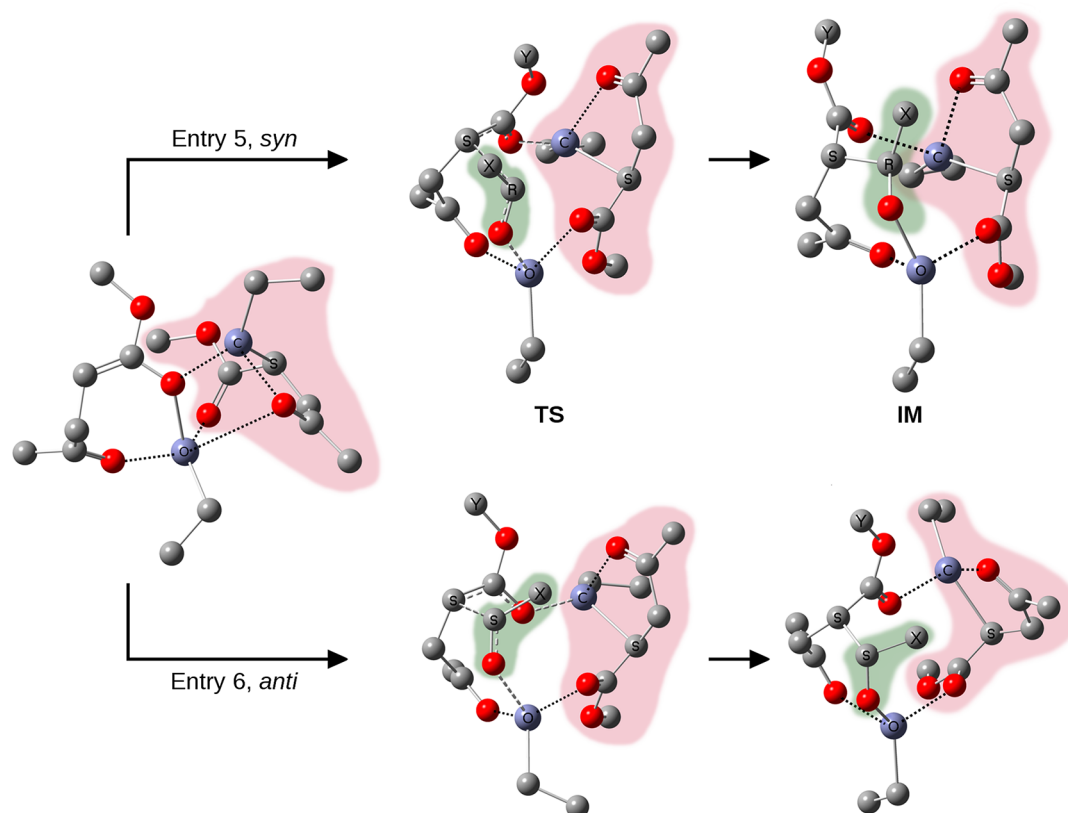


Figure 7. Most probable reaction pathway yielding *syn* and its equivalent reaction to *anti* intermediate (entries 5 and 6, Table 4). For simplification, hydrogens are not depicted. Gray, carbon; red, oxygen; blue, zinc. S, R: configuration at carbon centers; C, O: Zn^C, Zn^O. Green layer, acetaldehyde; red layer, unreactive keto-configured monomer.

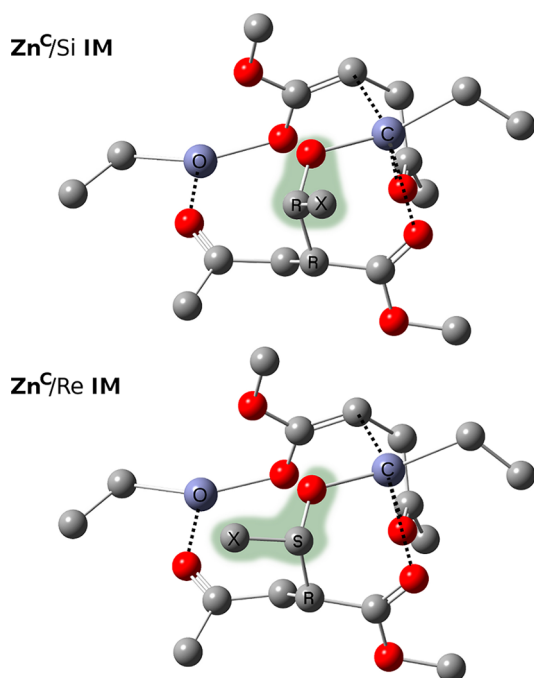


Figure 8. Intermediate products (IM) of entries 1 and 2 (Table 4). For simplification, hydrogens are not depicted. Gray, carbon; red, oxygen; blue, zinc. S, R: configuration at carbon centers; C, O: Zn^C, Zn^O. Green layer: acetaldehyde.

anti and *syn* configured species is formally conceivable by a keto–enol tautomerization of the carboxyl group adjacent to

the asymmetric center. However, the calculated energies of these enolate structures are 80–100 kJ/mol higher than the keto form because of lost Zn–O coordination interactions. Thus, the influence of such equilibrium effects on the *syn:anti* ratio can be neglected.

Computational investigations of the reaction up to the point of a protic quench reveal that the *syn* products would be favored because of a sterically controlled kinetic preference (Table 4, entry 5). The alkoxide intermediate derived from this aldol pathway is also the most stable intermediate and is the sole exergonic pathway as determined computationally. As the experimental results show the formation of both *syn* and *anti* aldol products, the intermediates reaction free energies of entries 1 and 2 (Table 4) appear to be overestimated, but exergonic values are still in the range of accuracy of the method used. However, the calculations provide additional support for the involvement of the ketone in biasing the reactivity of the intermediate to favor formation of the *syn* isomer.

CONCLUSION

Results of the NMR study for the TCA reaction of methyl pivaloylacetate **26** confirmed that the intermediate arising from the chain extension reaction possesses a carbon-bound zinc organometallic (**28**). The ¹H NMR and ¹³C NMR chemical shifts for this intermediate have been assigned with the use of deuterium labeling experiments, DEPT and 2D experiments. A control study involving traditional Reformatsky reactions confirmed that the *syn*-selectivity of the TCA reaction is dependent upon the presence of a γ -keto group in the TCA intermediate (**6**). Furthermore, studies performed in the

presence of tetrahydrofuran (THF), a donor molecule, provided additional evidence that γ -keto-Zn²⁺ complexation is associated with the observed *syn*-selectivity of the TCA reaction. Finally, studies in which the concentration of the reaction is varied suggest strongly that the *syn*-selectivity in the aldol reaction can be enhanced by decreasing the intermolecular complexation of the proposed organometallic dimer by using dilute reaction mixtures.

DFT calculations revealed that a reaction pathway from a dimeric species is probable and that the preference of the *syn*-product is related to intrinsic steric repulsion effects resulting from the different configurations involved in the aldehyde's reaction pathways. Additionally, the *E*-enolate was found not to be stable because of the short interatomic distance between the double bond and the zinc ion Z^O. The selectivity is predetermined by the asymmetric character of the *Z*-enolate **17b**, which includes both an enol monomer unit and a keto monomer. Two sides of the double bond (**17b**) are available for approach by the electrophilic aldehyde. The inherent asymmetry of the reacting aldehyde determines the lower reaction free energy leading to a *syn*-product.

The above studies confirm the unique diastereocontrol in the TCA reaction. A strategy for controlling zinc-aldol reactions through the presence of an appropriately positioned Lewis base can be inferred from these data. Additionally, this enhanced understanding of the intermediate formed in the zinc carbenoid-mediated chain extension reaction may facilitate the development of additional stereocontrolled tandem reactions.

EXPERIMENTAL SECTION

Preparative scale reactions were run in oven-dried glassware and stirred with Teflon-coated stir-bars. NMR studies were performed directly in NMR tubes. The terms concentrated in vacuo or under reduced pressure refer to the use of a rotary evaporator or vacuum pump.

Tetrahydrofuran (THF) was distilled from purple benzophenone ketyl prior to use. Benzene was distilled from calcium hydride prior to use. Methylene chloride (CH₂Cl₂) was distilled from P₂O₅ prior to use. Ethyl acetate (EtOAc) and hexanes were distilled prior to use. Pyridine was distilled from calcium hydride and stored over potassium hydroxide. Triethylamine (Et₃N) was distilled from potassium hydroxide.

Diethylzinc was purchased both as a solution (1.0 M in hexanes) and neat (as used for NMR studies). Methylene iodide (CH₂I₂) was stabilized through the addition of nonoxidized copper wire. Iodine was sublimed prior to use. Other reagents were used as received from commercial sources.

Column chromatography was performed with flash silica gel (32–63 μ m). Mobile phases were used as noted. Thin layer chromatography (TLC) was performed on glass plates and visualized by UV and anisaldehyde stain.

Nuclear magnetic resonance (NMR) spectroscopy was performed at 360.130 MHz for ¹H nuclei and 90.55 MHz for ¹³C nuclei, at 399.130 MHz for ¹H nuclei and 100.55 MHz for ¹³C nuclei, or at 499.766 MHz for ¹H nuclei and 125.679 MHz for ¹³C nuclei. All ¹³C were performed with ¹H-decoupling. Unless otherwise noted, all NMR experiments were carried out in deuteriochloroform (CDCl₃), which was stored over 4 Å molecular sieves, or dideuteromethylene chloride (CD₂Cl₂). All chemical shifts are reported in parts per million (ppm) and referenced to the resonance for CDCl₃ (¹H NMR δ 7.26 ppm; ¹³C NMR δ 77.16 (\pm 0.20) ppm). Unless otherwise noted, DEPT spectra are DEPT-135.

Methyl 2-iodo-5,5-dimethyl-4-oxo-hexanoate (20). An oven-dried 250-mL round-bottomed flask, equipped with a stir bar and a N₂ gas inlet, was charged with methylene chloride (40 mL) and

methylene iodide (1.6 mL, 20.0 mmol) and then cooled in an ice–water bath (0 °C). Diethylzinc (1 M) in hexanes (20 mL, 20.0 mmol) was added, and the resulting white suspension was stirred for 10 min. Methyl pivaloylacetate **26** (0.64 mL, 4.0 mmol) was added via syringe, and the reaction was allowed to stir at 0 °C for 30 min, at which time iodine (6.00 g, 23.7 mmol) was added to the mixture in a single portion. After a pink color developed and persisted for more than 30 s, the mixture was treated with a saturated aqueous solution of sodium thiosulfate (40 mL). After the pink color disappeared, a concentrated aqueous solution of ammonium chloride (40 mL) was added to the stirring suspension. The resulting mixture was extracted twice with diethyl ether (2 \times 70 mL). The combined organic layers were dried with sodium sulfate, filtered, and concentrated on a rotary evaporator. The crude oil was purified by flash column chromatography (10% ethyl acetate in hexanes) to yield methyl 2-iodo-5,5-dimethyl-4-oxo-hexanoate **20** (1.028 g, 86%) as a yellow oil. Trace amounts of chain extended material (methyl 5,5-dimethyl-4-oxo-hexanoate (**30**)) and the α,β -unsaturated ester (methyl 5,5-dimethyl-4-oxo-hex-2-enoate) were observed in the ¹H NMR spectrum: ¹H NMR (400 MHz, CD₂Cl₂, referenced to TMS 0.00 ppm) δ 4.57 (dd, 1H, *J* = 9.9, 5.0 Hz), 3.63 (s, 3H), 3.43 (dd, 1H, *J* = 18.2, 9.9), 3.07 (dd, 1H, *J* = 18.2, 5.0), 1.05 (s, 9H); ¹³C NMR (100 MHz, referenced to CD₂Cl₂ at 53.61 ppm) δ 213.1, 171.8, 53.0, 44.6, 43.8, 26.2, 12.3; HRMS-ESI *m/z* calcd for C₉H₁₆IO₃ [*M*⁺ + *H*] 299.0144, found 299.0148.

Methyl 2-(Hydroxy-(phenylmethyl))-5,5-dimethyl-4-oxo-hexanoate (22 and 23). An oven-dried round-bottomed flask, equipped with a stir bar and N₂ gas inlet, was charged with methyl 2-iodo-5,5-dimethyl-4-oxo-hexanoate **20** (0.1489 g, 0.50 mmol) in methylene chloride (2 mL) and cooled in an ice–water bath (0 °C). The solution was treated with diethyl zinc (1 M) in hexanes (0.5 mL, 0.50 mmol), and after stirring for 10 min, the reaction mixture was treated with methylene iodide (0.04 mL, 0.50 mmol). After stirring for an additional 20 min, benzaldehyde (0.15 mL, 1.50 mmol) was added. After 1 h, the reaction was quenched with saturated aqueous ammonium chloride (5 mL) and extracted twice with ethyl acetate (2 \times 30 mL). The combined organic layers were dried with sodium sulfate, decanted from sodium sulfate, and concentrated on rotary evaporator. The oily residue was subjected to column chromatography (5% ethyl acetate in hexanes) to yield a mixture of the aldol products, 2-(hydroxy-(phenylmethyl))-5,5-dimethyl-4-oxo-hexanoic acid methyl ester **22** and **23** (0.030 g, 21%) as a yellow oil. The *syn:anti* ratio resulting from the reaction, 7:1, was determined from integration of the ¹H NMR spectrum of the crude product mixture. The identities of the products were confirmed by comparing NMR spectra to results obtained by Lai et al.⁷ Methyl 5,5-dimethyl-4-oxo-hexanoate **30** was a byproduct of this reaction.

Methyl 2-iodo-5,5-dimethylhexanoate (21). An oven-dried 250-mL round-bottomed flask was equipped with a stir bar and charged with methylene chloride (90 mL), 3,3-dimethylbutanol (1.36 g, 10.39 mmol), *N*-methylmorpholine *N*-oxide (1.404 g, 10.39 mmol), and crushed 4 Å molecular sieves (5 g). The suspension was cooled to 0 °C and then treated with tetra-*N*-propylammonium peruthenate (TPAP) (0.183 g, 0.52 mmol). The reaction was monitored by thin layer chromatography and, upon completion, filtered under a vacuum through a plug of silica and Celite. The filter cake was rinsed with THF (200 mL), and the combined methylene chloride and THF-filtrates containing 3,3-dimethylbutan-1-ol was used in the next step.

An oven-dried round-bottomed flask, equipped with a stir bar, was charged with a solution of trimethylphosphonoacetate (3.78 g, 20.78 mmol) in THF (100 mL) at 0 °C under N₂ gas. This clear solution was treated with *n*-butyl lithium (2.5 M) in hexanes (8.31 mL, 20.78 mmol). After 30 min, the THF/methylene chloride solution of 3,3-dimethylbutan-1-ol **32** was added to the reaction. The mixture was allowed to warm to room temperature and monitored by TLC. After completion of the reaction, approximately 1 h, the reaction was quenched with saturated aqueous ammonium chloride (100 mL) and extracted with twice with diethyl ether (2 \times 100 mL). The organic layer was dried over sodium sulfate, vacuum filtered through Celite and concentrated on rotary evaporator. The crude oil was purified by flash column chromatography (1% ethyl acetate in hexane, *R_f* = 0.14)

to yield a mixture of *E* and *Z* methyl 5,5-dimethylhex-2-enoate (0.962 g, 59%) as a colorless oil (*E:Z*; 8:1).

E-isomer: ^1H NMR (400 MHz, CDCl_3) δ 6.96 (dt, 1H, $J = 15.6$, 7.8 Hz), 5.77 (d, 1H, 15.6 Hz), 3.69 (s, 3H), 2.05 (dd, 2H, $J = 7.8$, 1.0 Hz), 0.89 (s, 9H); ^{13}C NMR (400 MHz) δ 167.1, 147.3, 122.9, 51.5, 46.9, 29.5. *Z*-isomer: ^1H NMR (400 MHz, CDCl_3) δ 6.27 (dt, 1H, $J = 10.4$, 7.7 Hz), 5.81 (d, 1H, $J = 10.4$ Hz), 3.66 (s, 3H), 2.06 (dd, 2H, $J = 7.7$, 1.6 Hz), 0.89 (s, 9H); ^{13}C NMR (400 MHz) δ 167.1, 148.1, 120.6, 51.5, 42.4, 31.5; HRMS-ESI (mixture of *E* and *Z* isomers) m/z calcd for $\text{C}_9\text{H}_{17}\text{O}_2$ [$\text{M}^+ + \text{H}$] 157.1229, found 157.1226.

A round-bottomed flask, equipped with a stir bar, was charged with a mixture of *E* and *Z* isomers of methyl 5,5-dimethyl hex-2-enoate (0.962 g, 6.16 mmol) in THF (15 mL) and 10% Pd/C catalyst (0.096 g). The black suspension was stirred under a blanket of N_2 gas for approximately 10 min. With the N_2 gas inlet still connected and the flask under a positive nitrogen pressure, the suspension was purged with H_2 gas via a balloon. After a positive flow of H_2 gas through the N_2 gas bubbler was observed, the N_2 gas inlet was removed, and the reaction mixture was stirred with the balloon of H_2 gas attached. After 18 h, the balloon was removed, and the suspension was filtered by gravity filtration. The filtrate was concentrated on a rotary evaporator to yield methyl 5,5-dimethylhexanoate (0.611 g, 63%) as a colorless oil: ^1H NMR (400 MHz, CDCl_3) δ 3.67 (s, 3H), 2.28 (t, 2H, $J = 7.5$ Hz), 1.59 (m, 2H), 1.19 (m, 2H), 0.89 (s, 9H); ^{13}C NMR (400 MHz) δ 174.4, 51.6, 43.7, 35.0, 30.4, 29.4, 20.4; HRMS-ESI m/z calcd for $\text{C}_9\text{H}_{19}\text{O}_2$ [$\text{M}^+ + \text{H}$] 159.1385, found 159.1387.

An oven-dried round-bottomed flask equipped with a stir bar was charged with diisopropylamine (1.01 mL, 7.20 mmol) in THF (5 mL). Under N_2 gas, the solution was cooled in an ice–water bath (0 °C) and treated with *n*-butyllithium (2.5 M) in hexanes (2.6 mL, 6.50 mmol). The resulting clear, pale yellow solution was allowed to stir for 30 min and then cooled to –78 °C. Methyl 5,5-dimethylhexanoate (0.3845 g, 2.40 mmol) in THF (2 mL) was slowly added to the cooled solution, and after 1 h, a single portion of iodine (1.65 g, 6.50 mmol) was added to the enolate. After 18 h, the reaction was quenched with concentrated sodium thiosulfate (15 mL) and allowed to stir until the pink color disappeared. Concentrated aqueous ammonium chloride (10 mL) was added to the resulting mixture, which was then extracted twice with ethyl ether (2 × 50 mL). The combined organic layers were dried over sodium sulfate, filtered, and concentrated on a rotary evaporator to yield the crude product. The crude material was purified by column chromatography (100% hexane) to yield methyl 2-iodo-5,5-dimethylhexanoate **21** (0.326 g, 48%) as a pale yellow oil: ^1H NMR (400 MHz, CDCl_3) δ 4.24 (t, 1H, $J = 7.6$), 3.76 (s, 3H), 1.96 (m, 2H), 1.31 (m, 1H), 1.13 (m, 1H), 0.89 (s, 9H); ^{13}C NMR (100 MHz) δ 172.2, 53.0, 43.7, 32.1, 30.5, 29.8, 21.6; HRMS-ESI m/z calcd for $\text{C}_9\text{H}_{17}\text{I}\text{NaO}_2$ [$\text{M}^+ + \text{Na}$] 307.0171, found 307.0167.

Methyl 2-(hydroxy-phenyl-methyl)-5,5-dimethylhexanoate (24 and 25). An oven-dried round-bottomed flask, equipped with a stir bar, was charged with methyl 2-iodo-5,5-dimethyl-hexanoate **21** (0.1425 g, 0.50 mmol) in methylene chloride (5 mL) at 0 °C under N_2 gas. The solution was treated with diethyl zinc (1 M) in hexanes (0.5 mL, 0.50 mmol), and after stirring for 10 min, the reaction mixture was treated with methylene iodide (0.04 mL, 0.50 mmol). After stirring for an additional 20 min, benzaldehyde (0.15 mL, 1.50 mmol) was added. After 1 h, the reaction was quenched with saturated aqueous ammonium chloride (5 mL) and extracted twice with ethyl acetate (2 × 30 mL). The combined organic layer was dried with sodium sulfate, decanted from sodium sulfate, and concentrated on a rotary evaporator. The oily residue was subjected to column chromatography (7.5% ethyl acetate in hexanes) to yield a mixture of the aldol products, methyl 2-(hydroxy-phenyl-methyl)-5,5-dimethyl-hexanoate **24** and **25** (0.0524 g, 39%). Byproducts of this reaction included methyl 2-iodomethyl-5,5-dimethyl-hexanoate and methyl 5,5-dimethylhexanoate **35**. The *syn:anti* ratio of the aldol products, 1.6:1, was determined from integration of the resonance for the benzylic methine in the ^1H NMR spectrum of the crude product. The assignments of the *syn* and *anti* isomers were based upon vicinal coupling constants of the resonances at 4.92 and 4.79 ppm.^{7,15} **24** and **25**: ^1H NMR (400 MHz, CDCl_3) δ 7.37–7.28 (m, 10H), 4.92 (d, 1H, $J = 6.1$ Hz), 4.79

(d, 1H, $J = 7.7$ Hz), 3.68 (s, 3H), 3.57 (s, 3H), 2.96 (b, 1H), 2.80 (b, 1H), 2.73–2.63 (m, 2H), 1.85–1.48 (m, 4H), 1.39–1.22 (m, 2H), 1.02 (m, 2H), 0.83 (s, 9H), 0.78 (s, 9H); ^{13}C NMR (100 MHz, CDCl_3) δ 175.9, 175.5, 142.1, 141.8, 128.6, 128.5, 128.1, 127.9, 126.5, 126.3, 75.4, 74.6, 53.9, 53.7, 51.8, 51.7, 41.8, 41.2, 30.4, 30.3, 29.3, 29.2, 24.8, 22.6; HRMS-ESI m/z calcd for $\text{C}_{16}\text{H}_{25}\text{O}_3$ [$\text{M}^+ + \text{H}$] 265.1804, found 265.1807

Zinc-Organometallic Intermediate (28). An NMR tube was rinsed with acetone and hexane. After drying with a flow of N_2 gas, the NMR tube was fitted with a rubber septum and a N_2 gas inlet. A solution of methyl pivaloylacetate **26** (37 μL , 0.24 mmol) in CDCl_3 (0.7 mL) was introduced into the NMR tube. After observing the clear solution by ^1H and ^{13}C NMR spectroscopy, the mixture was again placed under N_2 gas and treated with neat diethyl zinc (50 μL , 0.48 mmol). With addition of diethyl zinc, the resulting mixture became warm but soon cooled to room temperature. An additional seal of parafilm treated with a drop of hexanes was wrapped around the rubber septum. The zinc-enolate was observed by ^1H and ^{13}C NMR spectroscopy.

Zinc-enolate of methyl pivaloylacetate: ^1H NMR (400 MHz, CDCl_3) δ 5.13 (s, 1H), 3.69 (s, 3H), 1.17 (s, 9H), 1.14 (t, 9H, $J = 8.1$ Hz), 0.26 (q, 6H, $J = 8.1$ Hz); ^{13}C NMR (100 MHz, CDCl_3) δ 196.0, 175.4, 85.9, 51.7, 40.1, 28.4, 10.8, 3.9 [ethane: ^1H NMR (400 MHz, CDCl_3) δ 0.85 (s); ^{13}C NMR (100 MHz, CDCl_3) δ 6.8]. The zinc-enolate mixture was placed under N_2 gas before treatment with methylene iodide (39 μL , 0.48 mmol), the addition of which resulted in slight effervescence and warming of the resulting pale yellow mixture. The parafilm used to wrap the tube was sealed using a drop of hexanes, and the pale yellow mixture was studied with various NMR-experiments (^1H NMR, ^{13}C NMR, 2D-NMR, and D-NMR experiments).

Zinc-organometallic intermediate (**28**): ^1H NMR (400 MHz, CDCl_3) δ 3.70 (s, 3H), 3.25 (flat b, 2H), 2.66 (b, 1H), 1.24 (s, 9H); ^{13}C NMR (100 MHz, CDCl_3) δ 230.0, 184.9, 53.8, 44.1, 38.5, 34.9, 26.7; [ethyl iodide: ^1H NMR (400 MHz, CDCl_3) δ 3.17 (q, 2H, $J = 7.5$ Hz), 1.82 (t, 3H, $J = 7.5$ Hz); ^{13}C NMR (100 MHz, CDCl_3) δ 20.7, –0.7]; [XZnCH_2]: ^1H NMR (400 MHz, CDCl_3) δ 1.69 (b); ^{13}C NMR (100 MHz, CDCl_3) δ –12.6 (b)].¹⁶

Computational Methods. All calculations reported in this body of work were performed using the program package Gaussian09, Revision A.01.¹⁷ As the literature demonstrated good results,¹⁸ the method consisting of the hybrid meta-GGA DFT functional M05–2X¹⁹ combined with the 6-311+G(2d,2p) basis set as implemented in Gaussian03 was used throughout. This basis set describes the second row atoms by the McLean–Chandler basis,²⁰ the basis set of McGrath and Curtiss²¹ for third row atoms, and the Watchers–Hay²² basis set for the first row of transition metals using the scaling factors of Raghavachari and Trucks.²³ As recommended when calculating transition metals, diffuse and polarized functions were used. All stationary points were characterized with a frequency analysis, where minima must have no imaginary frequencies and the saddle points have exactly one imaginary frequency. All given energies are free Gibbs energies (in kJ/mol) relative to the free and separated educts, which are zero point and thermally corrected. Therefore, all reported energetic values refer to standard conditions such as 298 K and 1 atm pressure.

Solvent corrected geometries and free energies were calculated with C-PCM as implemented in Gaussian03.²⁴ In this model, the species of interest are embedded in a cavity of molecular shape surrounded by a polarizable continuum, whose field modifies the energy and physical properties of the solute. The solvent reaction field is described by polarization charges distributed on the cavity surface. This procedure is known to reproduce experimental solvation energies reasonably well. Parameters for dichloromethane were chosen since this was the solvent used for the experimental investigations.

■ ASSOCIATED CONTENT

■ Supporting Information

Calculated energies and geometries, and ^1H and ^{13}C NMR spectra recorded in the preparation **20**, **21**, **24**, **25**, and **28**. This material is available free of charge via the Internet at <http://pubs.acs.org>.

■ AUTHOR INFORMATION

Corresponding Author

*E-mail: ckz@cisunix.unh.edu.

Notes

The authors declare no competing financial interest.

■ ACKNOWLEDGMENTS

We acknowledge Professor Gary Weisman and Kathleen Gallagher for advice and assistance with the NMR studies. We also acknowledge NIH (R15 GM060967) and the Pfizer Fellowship Supporting Diversity in Organic Chemistry for support of this research. The authors thank The University of Queensland for financial support.

■ REFERENCES

- (1) Brogan, J. B.; Zercher, C. K. *J. Org. Chem.* **1997**, *62*, 6444.
- (2) (a) Verbicky, C. A.; Zercher, C. K. *J. Org. Chem.* **2000**, *65*, 5615. (b) Hilgenkamp, R.; Zercher, C. K. *Tetrahedron* **2001**, *57*, 8793.
- (3) Reissig, H.-U.; Zimmer, R. *Chem. Rev.* **2003**, *103*, 1151.
- (4) Eger, W. A.; Zercher, C. K.; Williams, C. M. *J. Org. Chem.* **2010**, *75*, 7322.
- (5) Hilgenkamp, R.; Zercher, C. K. *Org. Lett.* **2001**, *3*, 3037.
- (6) Ronsheim, M. D.; Zercher, C. K. *J. Org. Chem.* **2003**, *68*, 1878.
- (7) Lai, S.; Zercher, C. K.; Jasinski, J. P.; Reid, S. N.; Staples, R. J. *Org. Lett.* **2001**, *3*, 4169.
- (8) (a) Brückner, C.; Lorey, H.; Reißig, H.-U. *Angew. Chem.* **1986**, *98*, 559. (b) Reißig, H.-U.; Reichelt, I.; Lorey, H. *Liebigs Ann. Chem.* **1986**, *1986*, 1924.
- (9) (a) Heim, R.; Wiedemann, S.; Williams, C. M.; Bernhardt, P. V. *Org. Lett.* **2005**, *7*, 1327. (b) Tilly, D. P.; Williams, C. M.; Bernhardt, P. V. *Org. Lett.* **2005**, *7*, 5155. (c) Schwartz, B. D.; Tilly, D. P.; Heim, R.; Wiedemann, S.; Williams, C. M.; Bernhardt, P. V. *Eur. J. Org. Chem.* **2006**, *2006*, 3181.
- (10) (a) Theberge, C. R.; Zercher, C. K. *Tetrahedron* **2003**, *59*, 1521. (b) Tryder, N. M.S. Thesis, University of Hampshire, 2003; (c) Lin, W.; Tryder, N.; Su, F.; Zercher, C. K.; Jasinski, J. P.; Butcher, R. J. *J. Org. Chem.* **2006**, *71*, 8140.
- (11) (a) Orsini, F.; Pelizzoni, F.; Ricca, G. *Tetrahedron Lett.* **1982**, *23*, 3945. (b) Dekker, J.; Boersma, J.; van der Kerk, G. J. M. *J. Chem. Soc., Chem. Commun.* **1983**, 553.
- (12) Dewar, M. J. S.; Metz, K. M., Jr. *J. Am. Chem. Soc.* **1987**, *109*, 6553.
- (13) (a) Heathcock, C. H. In *Asymmetric Synthesis*; Morrison, J. D., Ed.; Academic Press: New York, 1984; Vol. 3, p 111; (b) Tagliavini, E.; Trombini, C.; Umani-Ronchini, A. In *Advances in Carbanion Chemistry*; Snieckus, V., Ed.; JAI Press Inc.: Greenwich, 1996; Vol. 2, p 111.
- (14) Ronsheim, M. D.; Hilgenkamp, R.; Zercher, C. K. *Org. Synth.* **2002**, *79*, 146.
- (15) (a) Stiles, M.; Winkler, R. R.; Chang, Y.; Trayner, L. *J. Am. Chem. Soc.* **1964**, *86*, 3337. (b) House, H. O.; Crumrine, D. S.; Teranishi, A. Y.; Olmstead, H. D. *J. Am. Chem. Soc.* **1973**, *95*, 3310.
- (16) Charette, A. B.; Marcoux, J.-F. *J. Am. Chem. Soc.* **1996**, *118*, 4539.
- (17) *Gaussian 09*, Revision A.01; Frisch, M. J.; Trucks, G. W.; Schlegel, H. B.; Scuseria, G. E.; Robb, M. A.; Cheeseman, J. R.; Scalmani, G.; Barone, V.; Mennucci, B.; Petersson, G. A.; Nakatsuji, H.; Caricato, M.; Li, X.; Hratchian, H. P.; Izmaylov, A. F.; Bloino, J.; Zheng, G.; Sonnenberg, J. L.; Hada, M.; Ehara, M.; Toyota, K;

- Fukuda, R.; Hasegawa, J.; Ishida, M.; Nakajima, T.; Honda, Y.; Kitao, O.; Nakai, H.; Vreven, T.; Jr., J. A. M.; Peralta, J. E.; Ogliaro, F.; Bearpark, M.; Heyd, J. J.; Brothers, E.; Kudin, K. N.; Staroverov, V. N.; Kobayashi, R.; Normand, J.; Raghavachari, K.; Rendell, A.; Burant, J. C.; Iyengar, S. S.; Tomasi, J.; Cossi, M.; Rega, N.; Millam, J. M.; Klene, M.; Knox, J. E.; Cross, J. B.; Bakken, V.; Adamo, C.; Jaramillo, J.; Gomperts, R.; Stratmann, R. E.; Yazyev, O.; Austin, A. J.; Cammi, R.; Pomelli, C.; Ochterski, J. W.; Martin, R. L.; Morokuma, K.; Zakrzewski, V. G.; Voth, G. A.; Salvador, P.; Dannenberg, J. J.; Dapprich, S.; Daniels, A. D.; Farkas, Ö.; Foresman, J. B.; Ortiz, J. V.; Cioslowski, J.; Fox, D. J., Eds.; Gaussian, Inc.: Wallingford CT, 2009.
- (18) (a) Zhao, Y.; Truhlar, D. G. *Org. Lett.* **2006**, *8*, 5753. (b) Zhao, Y.; Truhlar, D. G. *J. Phys. Chem. A* **2006**, *110*, 5121. (c) Zhao, Y.; Truhlar, D. G. *Acc. Chem. Res.* **2008**, *41*, 157. (d) Sorkin, A.; Truhlar, D. G.; Amin, E. A. *J. Chem. Theory Comput.* **2009**, *5*, 1254.
- (19) Zhao, Y.; Schultz, N. E.; Truhlar, D. G. *J. Chem. Theory Comput.* **2006**, *2*, 364.
- (20) (a) Krishnan, R.; Binkley, J. S.; Seeger, R.; Pople, J. A. *J. Chem. Phys.* **1980**, *72*, 650. (b) McLean, A. D.; Chandler, G. S. *J. Chem. Phys.* **1980**, *72*, 5639.
- (21) (a) Binning, R. C. J.; Curtiss, L. A. *J. Comput. Chem.* **1990**, *11*, 1206. (b) McGrath, M. P.; Radom, L. *J. Chem. Phys.* **1991**, *94*, 511. (c) Curtiss, L. A.; McGrath, M. P.; Blauddau, J.-P.; Davis, N. E.; Robert, C.; Binning, J.; Radom, L. *J. Chem. Phys.* **1995**, *103*, 6104.
- (22) (a) Wachters, A. J. H. *J. Chem. Phys.* **1970**, *52*, 1033. (b) Hay, P. J. *J. Chem. Phys.* **1977**, *66*, 4377.
- (23) Raghavachari, K.; Trucks, G. W. *J. Chem. Phys.* **1989**, *91*, 1062.
- (24) (a) Klamt, A.; Schüürmann, G. *J. Chem. Soc., Perkin Trans. 2* **1993**, 799. (b) Barone, V.; Cossi, M. *J. Phys. Chem. A* **1998**, *102*, 1995. (c) Cossi, M.; Rega, N.; Scalmani, G.; Barone, V. *J. Comput. Chem.* **2003**, *24*, 669.